

***Chlamydomonas cpc1-1* mutant exhibits unexpected growth phenotypes**

Comparative analysis of *Chlamydomonas* strains revealed that a *cpc1-1* mutant has three unexpected growth phenotypes across different media types, suggesting possible genetic background contributions beyond characterized mutations.

Contributors (A-Z)

Audrey Bell, Megan L. Hochstrasser, Cameron Dale MacQuarrie, David G. Mets

Version 1 · May 22, 2025

Purpose

Chlamydomonas reinhardtii mutants with specific flagellar defects are important models for studying ciliary dysfunction in human disease [1]. We recently used two flagellar mutants, central pair complex mutant *cpc1-1* (CC-3707) and inner dynein arm mutant *ida4* (CC-2670) to model human diseases spermatogenic failure 43 and 83 [2], respectively, using motility as the phenotype of interest. In that study, we found multiple drugs that recovered upward motility and/or recovered aspects of single-cell swimming behavior. Since many of these drugs could impact cellular metabolism and metabolism can be probed by growth [2][3], we performed comparative growth

analysis of these mutants, along with control strains, across diverse media compositions to probe for metabolic phenotypes.

Our results reveal that *cpc1-1* exhibits three unexpected growth phenotypes: enhanced growth on proteose peptone-supplemented media, maintained chlorophyll production on nitrate-containing media (we'd expect production to be inhibited), and unique halotolerance on marine medium. In contrast, *ida4* behaves similarly to wild-type *C. reinhardtii* (CC-124), from which it derives. *cpc1-1* originates from mutagenesis in a distinct *nit-350* strain (CC-2677), after which the progeny with the *cpc1-1* allele was backcrossed with CC-124. Our findings suggest that *cpc1-1* may retain some genetic material from its parent strain (CC-2677) that impacts metabolism, and these growth phenotypes may be independent of the characterized central pair complex defects.

This work highlights the importance of considering genetic background effects and validating outcrossing.

Background and goals

Origin and characterization of the *cpc1-1* mutant

The *cpc1-1* mutant was initially generated through insertional mutagenesis using a nitrate reductase (NIT1)-selectable marker in a nitrate reductase-deficient host strain (*nit1-305*, CC-2677) [4]. The transformation approach resulted in a genomic insertion that disrupted the *CPC1* gene, which encodes a ~350 kDa protein localized to the central pair apparatus of the flagellar axoneme. Electron microscopy revealed that the *cpc1-1* mutation specifically disrupts the C1b projection of the central pair complex, leading to altered flagellar waveform and reduced swimming velocity [4].

Further biochemical analysis identified that CPC1 contains an adenylate kinase domain and interacts with enolase and other glycolytic enzymes, suggesting a potential role in local ATP regulation within the flagellar axoneme [5]. We recently reported that the motility defects in the *cpc1-1* strain can be reversed with drugs that may impact metabolism [2], but CPC1's role in metabolic pathways hasn't been explored.

Genetic background considerations

The *cpc1-1* mutation was generated in strain CC-2677 (*nit1-305*), a genetic lineage distinct from the widely used 137c laboratory background strains (CC-124/CC-125). After initial characterization, the *cpc1-1* mutation underwent backcrossing "at least four times" into the 137c background to generate the strain CC-3707 used for studies of central pair complex function [4][5]. While this recurrent backcrossing has likely incorporated the majority of the 137c genetic background (theoretically at least 94% after four backcrosses [6]), portions of the original CC-2677 genome will persist in the current CC-3707 strain. However, the 137c strain CC-124 remains the best wild-type control for *cpc1-1* since the majority of the mutant's genome is derived from the 137c lineage. The characteristic reduced flagellar beat frequency in this mutant was rigorously mapped to the *CPC1* locus through comprehensive genetic approaches, including multiple independent alleles exhibiting complementation failure [4], so we can safely infer causality between *CPC1* disruption and the observed motility defect.

The *ida4* mutant (CC-2670) exhibits a defect in the inner dynein arm I-projection resulting in the loss of specific dynein subspecies from the axoneme and reduced swimming velocity. Unlike *cpc1-1*, this mutation was introduced in the 137c background without extensive backcrossing from a divergent strain [7][8].

Chlamydomonas smithii (CC-1373) is fully interfertile with *C. reinhardtii* but has a distinct genetic background with significant sequence polymorphisms [9]. Importantly, unlike standard laboratory strains of *C. reinhardtii* (CC-124/CC-125), which carry *nit1* and *nit2* mutations preventing growth on nitrate as a sole nitrogen source, *C. smithii* retains functional nitrate assimilation pathways [10][11][12]. This strain, therefore, serves as a positive control for the ability to utilize nitrate.

Finally, *C. reinhardtii* strain CC-5415 (*nit1 agg1*) is a cross between *nit1-305* and CC-124 and we included it as an additional control because, like strain CC-3707, it contains genetic contributions from both *nit1-305* and 137c backgrounds. However, due to the multiple generations of backcrossing, CC-3707 retains a substantially higher proportion of the 137c genome than CC-5415.

Goals

We wanted to understand whether *ida4* and *cpc1-1* mutants exhibit growth phenotypes distinct from wild-type strains across various media compositions, indicative of metabolic defects. We sought to:

1. Characterize growth patterns of *cpc1-1* and *ida4* compared to wild-type strains on standard and nutrient-enriched media
2. Assess nitrogen utilization capabilities across different nitrogen sources

The approach

We compared growth of wild-type *Chlamydomonas smithii* (CC-1373) and *Chlamydomonas reinhardtii* (CC-124, CC-5415) strains, the *cpc1-1* mutant (CC-3707), and the *ida4* mutant (CC-2670) across multiple media formulations to identify metabolic influences of these mutations. We controlled for initial cell density to ensure precise quantification of growth differences. All strains were transferred to these different media after growth under the same culturing conditions to avoid environmental influences.

Strains and culture conditions

We examined growth for the following *Chlamydomonas* strains ([Table 1](#)).

Strain	Description	Species
CC-124	<i>nit1 nit2</i> mt- (lab background strain)	<i>C. reinhardtii</i>
CC-1373	Wild type mt+	<i>C. smithii</i>
CC-2670	<i>ida4</i> mt+	<i>C. reinhardtii</i>
CC-3707	<i>cpc1-1</i> mt-	<i>C. reinhardtii</i>
CC-5415	<i>nit1 agg1</i> mt+ (lab background strain)	<i>C. reinhardtii</i>

Table 1

***Chlamydomonas* strains we examined in this work.**

Additionally, we included the adenosine deaminase mutant strain CLIP2.048478 in the experiments. However, we didn't include these results in the text because we took cells directly from the *Chlamydomonas* Resource Center inoculum, not from a single colony we'd PCR-confirmed to have the mutant *ada* allele. Therefore, we can't claim that the *ada* mutant allele causes any potential growth phenotypes we observed. However, we include the data in a [supplemental figure](#).

We maintained all strains on standard TAP (tris-acetate-phosphate) medium with 1.5% agar under 12:12 light:dark cycles at ambient temperature.

Experimental setup and cell preparation

We harvested cells from TAP + 1.5% agar plates and suspended them in approximately 1 mL of liquid TAP medium. We passed all suspensions through 5 μ m filters via centrifugation to ensure uniform cell populations and eliminate aggregates.

We took initial optical density measurements at 730 nm using a SpectraMax iD3 plate reader (Molecular Devices) with samples loaded into a black-walled 96-well plate. We normalized cell suspensions to the lowest concentration ($OD_{730} = 0.043$) by diluting with TAP medium according to calculated ratios. We then maintained the plate under static conditions overnight with a 12:12 light:dark cycle.

Serial dilution and plating

The next day, we prepared serial dilutions (1:1, 1:10, 1:100, 1:1000, 1:10,000) of the normalized cell suspensions by successively transferring 30 μL aliquots into wells containing 270 μL of fresh TAP medium. For each strain and dilution, we spotted 2 μL onto solid media plates in triplicate (except for soil extract medium, which had two replicates due to contamination issues).

Growth media formulations

We tested growth across multiple media formulations to assess strain-specific responses to different nutrient compositions ([Table 2](#)).

Media	Age of plate at time of inoculation (months)	Replicates
TAP	4.3	3
AF6	2.5	3
Bristol	4.3	3
Modified Bold's 3N (MB3N)	4.0	3
M-N	5.5	3
Nutrient broth	8.2	3
Soil extract	4.2	2
TAP + 2.5% proteose peptone	9.5	3
Erdschreiber's	5.5	3

Table 2

Media we used to grow *Chlamydomonas* strains.

We prepared all media formulations with 1.5% agar and stored them at 4 °C until use. The age of the plates ranged from 4 to 10 months because we limited the

experimental design to readily available materials. Before inoculation, we equilibrated the plates to room temperature overnight.

TAP (tris-acetate-phosphate) media

375 μM NH_4Cl , 17.5 μM $\text{CaCl}_2 \cdot 2\text{H}_2\text{O}$, 20 μM $\text{MgSO}_4 \cdot 7\text{H}_2\text{O}$, 6 μM Na_2HPO_4 , 4 μM KH_2PO_4 , 200 μM Trizma base, 170 μM glacial acetic acid, with Hutner's trace elements solution at final concentration of 134 nM $\text{Na}_2\text{EDTA} \cdot 2\text{H}_2\text{O}$, 770 nM $\text{ZnSO}_4 \cdot 7\text{H}_2\text{O}$, 184 nM H_3BO_3 , 26 nM $\text{MnCl}_2 \cdot 4\text{H}_2\text{O}$, 18 nM $\text{FeSO}_4 \cdot 7\text{H}_2\text{O}$, 7 nM $\text{CoCl}_2 \cdot 6\text{H}_2\text{O}$, 5 nM $\text{CuSO}_4 \cdot 5\text{H}_2\text{O}$, and 0.8 nM $(\text{NH}_4)_6\text{Mo}_7\text{O}_{24} \cdot 4\text{H}_2\text{O}$. Suspended in ultrapure water. For TAP + 2.5% proteose peptone, we added 2.5% proteose peptone purchased from Millipore (Cat No 82450).

AF6 media

2 mM MES, 8.13 μM Fe-citrate, 10.4 μM citric acid, 1.65 mM NaNO_3 , 275 μM NH_4NO_3 , 122 μM $\text{MgSO}_4 \cdot 7\text{H}_2\text{O}$, 73.5 μM KH_2PO_4 , 28.7 μM K_2HPO_4 , 68 μM $\text{CaCl}_2 \cdot 2\text{H}_2\text{O}$, with trace elements (13.4 μM $\text{Na}_2\text{EDTA} \cdot 2\text{H}_2\text{O}$, 3.63 μM $\text{FeCl}_3 \cdot 6\text{H}_2\text{O}$, 0.91 μM $\text{MnCl}_2 \cdot 4\text{H}_2\text{O}$, 0.38 μM $\text{ZnSO}_4 \cdot 7\text{H}_2\text{O}$, 84.1 nM $\text{CoCl}_2 \cdot 6\text{H}_2\text{O}$, 51.7 nM $\text{Na}_2\text{MoO}_4 \cdot 2\text{H}_2\text{O}$) and vitamins (29.6 nM thiamine-HCl, 8.2 nM biotin, 5.9 nM pyridoxine-HCl, 0.74 nM cyanocobalamin). pH adjusted to 6.6. Suspended in ultrapure water.

Bristol

2.94 mM NaNO_3 , 0.17 mM $\text{CaCl}_2 \cdot 2\text{H}_2\text{O}$, 0.3 mM $\text{MgSO}_4 \cdot 7\text{H}_2\text{O}$, 0.43 mM K_2HPO_4 , 1.29 mM KH_2PO_4 , and 0.43 mM NaCl. Suspended in ultrapure fresh water.

Modified Bold's 3N (MB3N)

8.82 mM NaNO_3 , 0.17 mM $\text{CaCl}_2 \cdot 2\text{H}_2\text{O}$, 0.3 mM $\text{MgSO}_4 \cdot 7\text{H}_2\text{O}$, 0.43 mM K_2HPO_4 , 1.29 mM KH_2PO_4 , 0.43 mM NaCl, with P-IV trace metals (12 μM $\text{Na}_2\text{EDTA} \cdot 2\text{H}_2\text{O}$, 2.16 μM $\text{FeCl}_3 \cdot 6\text{H}_2\text{O}$, 1.26 μM $\text{MnCl}_2 \cdot 4\text{H}_2\text{O}$, 222 nM ZnCl_2 , 50.4 nM $\text{CoCl}_2 \cdot 6\text{H}_2\text{O}$, 102 nM $\text{Na}_2\text{MoO}_4 \cdot 2\text{H}_2\text{O}$) and vitamins (100 nM vitamin B12 (cyanocobalamin), 100 nM biotin, 1 μM thiamine). The final media has 4% pasteurized soil water supernatant (0.05 mM CaCO_3 , 2.5% greenhouse soil, suspended in ultrapure water and purchased from UTEX). pH adjusted to 6.2. Suspended in ultrapure water.

M-N

1.7 mM $\text{Na}_3\text{C}_6\text{H}_5\text{O}_7 \cdot 2\text{H}_2\text{O}$, 37 μM $\text{FeCl}_3 \cdot 6\text{H}_2\text{O}$, 360 μM $\text{CaCl}_2 \cdot 2\text{H}_2\text{O}$, 1.22 mM $\text{MgSO}_4 \cdot 7\text{H}_2\text{O}$, 1.32 mM $\text{K}_2\text{HPO}_4 \cdot 3\text{H}_2\text{O}$, with trace elements (16.2 μM H_3BO_3 , 3.5 μM $\text{ZnSO}_4 \cdot 7\text{H}_2\text{O}$, 1.8 μM $\text{MnSO}_4 \cdot \text{H}_2\text{O}$, 0.84 μM $\text{CoCl}_2 \cdot 6\text{H}_2\text{O}$, 0.83 μM $\text{Na}_2\text{MoO}_4 \cdot 2\text{H}_2\text{O}$, 0.28 μM $\text{CuSO}_4 \cdot 5\text{H}_2\text{O}$). pH adjusted to 6.8. Suspended in ultrapure water.

Nutrient broth

3.0 g/L beef extract and 5.0 g/L peptone. Purchased from Millipore (Cat No N7519). Suspended in ultrapure water.

Soil extract

96% Bristol media and 4% pasteurized soil water supernatant (0.05 mM CaCO_3 , 2.5% greenhouse soil, suspended in ultrapure water and purchased from UTEX).

Erdschreiber's

2.3 mM NaNO_3 , 67 μM $\text{Na}_2\text{HPO}_4 \cdot 7\text{H}_2\text{O}$, 23.7 μM $\text{Na}_2\text{EDTA} \cdot 2\text{H}_2\text{O}$, 4.3 μM $\text{FeCl}_3 \cdot 6\text{H}_2\text{O}$, 2.5 μM $\text{MnCl}_2 \cdot 4\text{H}_2\text{O}$, 400 nM ZnCl_2 , 100 nM $\text{CoCl}_2 \cdot 6\text{H}_2\text{O}$, 200 nM $\text{Na}_2\text{MoO}_4 \cdot 2\text{H}_2\text{O}$, 100 nM cyanocobalamin, and 50 μM HEPES. Suspended in synthetic seawater (409 mM NaCl , 53 mM $\text{MgCl}_2 \cdot 6\text{H}_2\text{O}$, 28 mM Na_2SO_4 , 10 mM $\text{CaCl}_2 \cdot 2\text{H}_2\text{O}$, 1 mM KCl , 1 mM NaHCO_3 , 1 mM KBr , 0.4 mM $\text{SrCl}_2 \cdot 6\text{H}_2\text{O}$, 1 mM H_3BO_3 , 3 mM NaOH , and 2 mM NaF [RICCA Chemical Company: R8363000]) and 4% pasteurized soil water supernatant (0.05 mM CaCO_3 , 2.5% greenhouse soil, suspended in ultrapure water and purchased from UTEX).

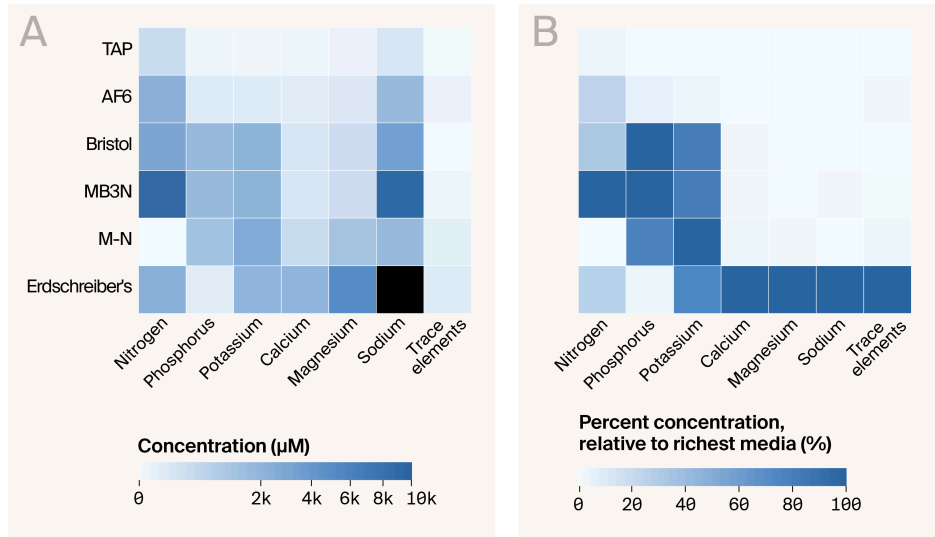


Figure 1

Comparative breakdown of media in this study.

(A) Absolute concentrations of major nutrients and trace elements in TAP, AF6, Bristol, MB3N, M-N, and Erdschreiber's media. Erdschreiber's sodium is black, indicating that the value is saturated and greater than 10,000 µM.

(B) Same data from (A) as percentages relative to the highest concentration for each nutrient. Crosshatched cells indicate the absence of a nutrient component.

Growth conditions and documentation

After spotting, we left the plates upright to dry overnight in a tent equipped with grow lights under 24 hours of illumination at ambient temperature. The next day, we inverted the plates and placed them in clear, plastic shoeboxes to maintain humidity and prevent desiccation. We kept the plates under constant illumination at ambient temperature throughout the experiment.

We recorded initial observations 12 days post-inoculation, with particular attention to the enhanced growth of CC-3707 on proteose peptone-supplemented medium. We

captured images using an Azure gel documentation system with Cy5 settings to visualize chlorophyll fluorescence as a proxy for colony growth and viability.

We performed comprehensive plate documentation at 20 days and 47 days post-inoculation using a standardized imaging setup consisting of a mini-light box on its side with a cardboard aperture to maintain consistent lighting across all plates. We acquired images with a Google Pixel 6 smartphone camera.

Pub preparation

We assembled the figures in Adobe Illustrator. We used Claude to help write code, reorganize text using a template, suggest wording ideas, and then chose which small phrases or sentence structure ideas to use, help copy-edit draft text to match Arcadia's style, help clarify and streamline text that we wrote, and write text that we edited. We generated the [Figure 1](#) heatmaps by converting concentrations to micromolar values using Python (v3.12.5) with NumPy (v2.1.2) and Pandas (v2.2.3) and plotted with Matplotlib (v3.9.2), Seaborn (v0.13.2), and arcadia-pycolor (v0.5.1) [13].

The observations

Our comparative growth analysis revealed distinctive phenotypic differences among the tested strains that appear unrelated to their characterized flagellar defects.

Enhanced growth on proteose peptone-supplemented medium

When we grew strains on standard TAP medium, we observed that the *cpc1-1* and *ida4* mutants exhibited a reduced colony density compared to wild-type CC-124 based on the chlorophyll intensity in the colonies ([Figure 2](#), left). However, we observed a striking pattern reversal for *cpc1-1* cells when we supplemented the medium with 2.5% proteose peptone (TAP+PP). On TAP+PP medium, *cpc1-1* colonies displayed substantially enhanced growth compared to wild-type CC-124 cells, achieving greater colony diameter and density than wild-type strains under the same conditions.

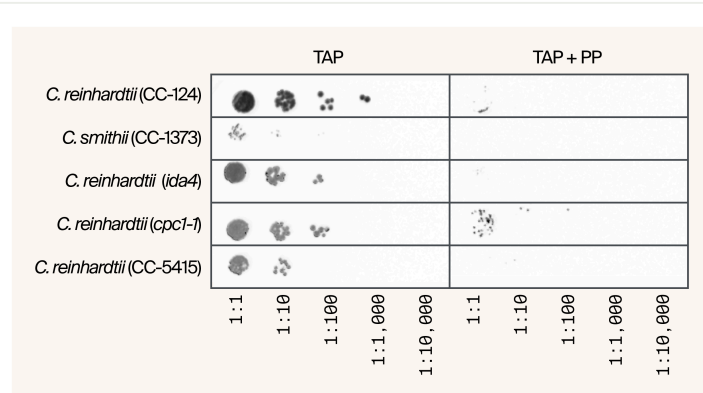


Figure 2

Enhanced growth of *cpc1-1* on proteose peptone-supplemented medium. Chlorophyll fluorescence images of serially diluted *Chlamydomonas* strains (dilutions from 1:1 to 1:10,000) grown on TAP medium (left) and TAP + 2.5% proteose peptone (right).

This differential response became evident within 12 days of inoculation and was pronounced by day 20 ([Figure 3](#)), as documented in our systematic imaging. Of note, the peptone in the media gave the agar a dark yellow hue. The *cpc1-1* mutant showed growth even at the 1:10 and 1:100 dilutions on TAP+PP, whereas wild-type strains and the *ida4* mutant showed little to no growth. The enhanced growth was consistent across all three replicates.

Retention of chlorophyll production on alternative nitrogen sources

We identified a second distinctive phenotype on media containing nitrate as the primary nitrogen source (AF6, Bristol, modified Bold's 3N, and soil extract media), in contrast to TAP medium, which uses ammonium as its nitrogen source. Wild-type *C. reinhardtii* CC-124, CC-5415, and the *ida4* mutant exhibited pronounced chlorosis on the nitrate-containing media, developing yellow colonies characteristic of strains with the *nit2* mutation in the 137c lineage. This mutation impairs nitrate utilization, leading to nitrogen starvation and chlorophyll degradation ([Figure 3](#)) [12].

In contrast, *cpc1-1* colonies maintained a dark-green coloration on these nitrate-containing media, similar to wild-type *C. smithii* (CC-1373), which has functional nitrate assimilation pathways. This unexpected chlorophyll retention suggests that *cpc1-1* may have kept functional *NIT2* alleles from its CC-2677 ancestry, enabling more efficient nitrogen utilization from nitrate sources.

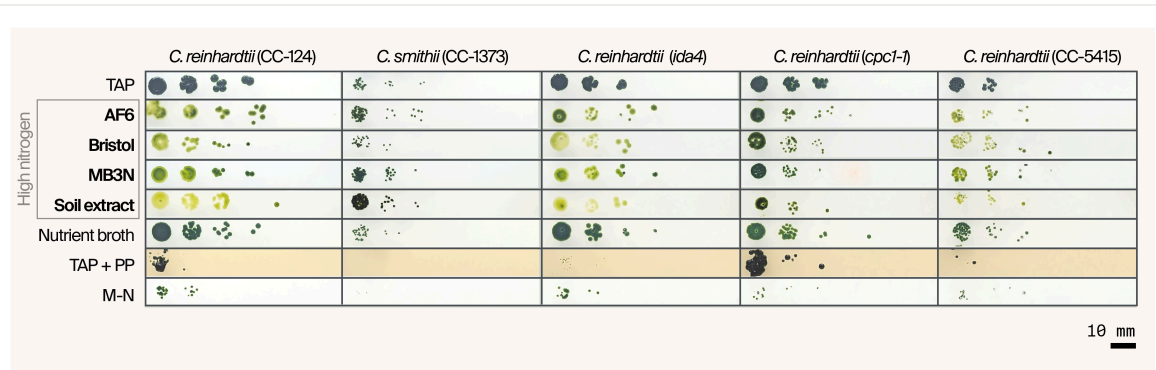


Figure 3

Comparative growth of *Chlamydomonas* strains across multiple media types at 20 days post-inoculation.

RGB images showing 20 days of growth of *C. reinhardtii* (WT: CC-124), *C. smithii* (WT: CC-1373), *C. reinhardtii* (*ida4*: CC-2670), *C. reinhardtii* (*cpc1-1*: CC-3707), and *C. reinhardtii* (WT: CC-5415) on eight different media types: TAP, AF6, Bristol, MB3N, soil extract, nutrient broth, TAP + 2.5% proteose peptone, and M-N.

Note the yellowing (chlorosis) of colonies for CC-124 and *ida4* on nitrate-containing media compared to the maintained green coloration in *cpc1-1*, *C. smithii*, and CC-5415, indicating functional nitrate assimilation pathways.

Halotolerance of *cpc1-1* on marine media

We discovered a third unexpected phenotype after extended growth periods. At 47 days post-inoculation, we observed that *cpc1-1* was the only strain capable of growing on Erdschreiber's marine medium with elevated salt content ([Figure 4](#)) ([Figure 1](#)). While all other strains showed no detectable growth on this medium, *cpc1-1* established a visible colony on two of the three plates, indicating a previously uncharacterized halotolerance phenotype. Though we've previously reported *C. smithii* growth on Erdschreiber's medium [10], we didn't observe that here after 47 days. So it's worth considering that colonies from other strains might appear on these plates over a more extended period, or if we'd used a denser starting culture, since we'd set these experiments up with dilute starter cultures.

This finding further supports that genetic elements in the *cpc1-1* strain differ from the standard 137c background and confer adaptive advantages under specific environmental conditions.

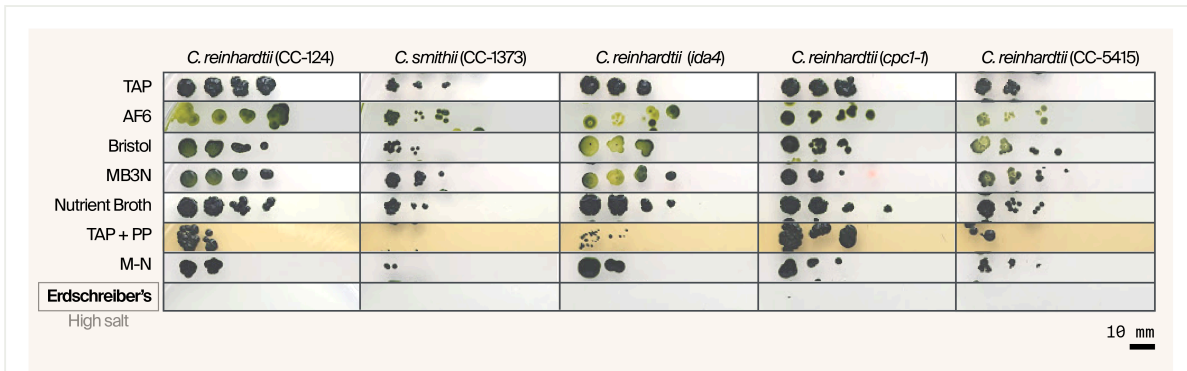


Figure 4

Extended growth analysis at 47 days post-inoculation, revealing halotolerance of *cpc1-1*.

RGB images showing 47 days of growth of *C. reinhardtii* (WT: CC-124), *C. smithii* (WT: CC-1373), *C. reinhardtii* (*ida4*: CC-2670), *C. reinhardtii* (*cpc1-1*: CC-3707), and *C. reinhardtii* (WT: CC-5415) on TAP, AF6, Bristol, MB3N, nutrient broth, TAP + 2.5% proteose peptone, M-N, and Erdschreiber's media. Note that only *cpc1-1* shows growth, albeit minimal, on Erdschreiber's medium (marine medium with elevated salt content), indicating a unique halotolerance phenotype. We didn't include soil extract medium because of contamination issues.

Thoughts and questions

Our comparative growth analysis reveals that the *cpc1-1* mutant (CC-3707) has three distinct phenotypes that differentiate it from the wild-type strains CC-124 and CC-5415 and the *ida4* mutant: enhanced growth on protein-rich media, maintained chlorophyll production when using nitrate as a nitrogen source, and unique halotolerance on marine medium. These characteristics could stem from genetic elements inherited from the original CC-2677 (*nit1-305*) background that persisted through backcrossing into the 137c lineage. However, none of these phenotypes were present in CC-5415, the product of a cross between *nit1-305* and a 137c background. Since CPC1 is known to interact with enolase and components of the metabolic machinery [5], it remains

possible that the *cpc1-1* allele causes these phenotypes; however, our current evidence isn't sufficient to draw conclusions.

To address this, we'll be taking a two-pronged approach. We've acquired strain CC-5148, which is derived from 137c strain CC-125 that spontaneously acquired a missense mutation preventing CPC1 protein from localizing to the flagella [14]. This mutant allele was named *cpc1-2*. We'll perform comparative studies on the growth of CC-5148 to determine if the *cpc1-2* mutation is sufficient to induce these growth phenotypes in a controlled background. However, since the mutation appears only to impact CPC1 localization, the protein may still be able to function in the cell body in this mutant, so CPC1-dependent metabolic phenotypes might not be apparent. As a second approach, we'll overexpress wild-type full-length CPC1 in both mutants to recover wild-type behavior independent of strain background.

Acknowledgements

Thank you to Hayley Greenough for providing the agar media plates used in this study.

References

- 1 Pazour GJ, Witman GB. (2009). The Chlamydomonas Flagellum as a Model for Human Ciliary Disease. <https://doi.org/10.1016/b978-0-12-370873-1.00052-6>
- 2 Essock-Burns T, Lane R, MacQuarrie CD, Mets DG. (2024). Rescuing Chlamydomonas motility in mutants modeling spermatogenic failure. <https://doi.org/10.57844/ARCADIA-FE2A-711E>
- 3 Sprague GF, Cronan JE. (1977). Isolation and characterization of Saccharomyces cerevisiae mutants defective in glycerol catabolism. <https://doi.org/10.1128/jb.129.3.1335-1342.1977>

- 4 Mitchell DR, Sale WS. (1999). Characterization of a *Chlamydomonas* Insertional Mutant that Disrupts Flagellar Central Pair Microtubule-associated Structures. <https://doi.org/10.1083/jcb.144.2.293>
 - 5 Zhang H, Mitchell DR. (2004). Cpc1, a *Chlamydomonas* central pair protein with an adenylate kinase domain. <https://doi.org/10.1242/jcs.01297>
 - 6 Hill WG. (1998). Selection with Recurrent Backcrossing to Develop Congenic Lines for Quantitative Trait Loci Analysis. <https://doi.org/10.1093/genetics/148.3.1341>
 - 7 Kamiya R, Kurimoto E, Muto E. (1991). Two types of *Chlamydomonas* flagellar mutants missing different components of inner-arm dynein. <https://doi.org/10.1083/jcb.112.3.441>
 - 8 Kamiya R. (1988). Mutations at twelve independent loci result in absence of outer dynein arms in *Chlamydomonas reinhardtii*. <https://doi.org/10.1083/jcb.107.6.2253>
 - 9 Flowers JM, Hazzouri KM, Pham GM, Rosas U, Bahmani T, Khraiweh B, Nelson DR, Jijakli K, Abdrabu R, Harris EH, Lefebvre PA, Hom EFY, Salehi-Ashtiani K, Purugganan MD. (2015). Whole-Genome Resequencing Reveals Extensive Natural Variation in the Model Green Alga *Chlamydomonas reinhardtii*. <https://doi.org/10.1105/tpc.15.00492>
 - 10 Avasthi P, Braverman B, Essock-Burns T, Garcia G, MacQuarrie CD, Matus DQ, Mets DG, York R. (2024). Phenotypic differences between interfertile *Chlamydomonas* species. <https://doi.org/10.57844/ARCADIA-35F0-3E16>
 - 11 Pröschold T, Harris EH, Coleman AW. (2005). Portrait of a Species. <https://doi.org/10.1534/genetics.105.044503>
 - 12 Fernández E, Matagne RF. (1986). In vivo complementation analysis of nitrate reductase-deficient mutants in *Chlamydomonas reinhardtii*. <https://doi.org/10.1007/bf00418413>
 - 13 arcadia-pycolor. (2025). <https://github.com/Arcadia-Science/arcadia-pycolor>
 - 14 Lin H, Guo S, Dutcher SK. (2018). RPGRIP1L helps to establish the ciliary gate for entry of proteins. <https://doi.org/10.1242/jcs.220905>
-